Structure−Activity Relationships of the p38α MAP Kinase Inhibitor 1-(5-*tert*-Butyl-2-*p*-tolyl-2*H*-pyrazol-3-yl)-3-[4-(2-morpholin-4-yl-ethoxy)naphthalen-1-yl]urea (BIRB 796)

John Regan,*,[†] Alison Capolino,[†] Pier F. Cirillo,[†] Thomas Gilmore,[†] Anne G. Graham,[‡] Eugene Hickey,[†] Rachel R. Kroe,[‡] Jeffrey Madwed,[§] Monica Moriak,[†] Richard Nelson,[†] Christopher A. Pargellis,[‡] Alan Swinamer,[†] Carol Torcellini,[§] Michele Tsang,[†] and Neil Moss[†]

Departments of Medicinal Chemistry, Immunology and Inflammation, and Pharmacology, Boehringer Ingelheim Pharmaceuticals, Research and Development Center, 900 Ridgebury Road, Ridgefield, Connecticut 06877

We report on the structure−activity relationships (SAR) of 1-(5-*tert*-butyl-2-*p*-tolyl-2*H*-pyrazol-3-yl)-3-[4-(2-morpholin-4-yl-ethoxy)naphthalen-1-yl]urea (BIRB 796), an inhibitor of p38α MAP kinase which has advanced into human clinical trials for the treatment of autoimmune diseases. Thermal denaturation was used to establish molecular binding affinities for this class of p38α inhibitors. The *tert*-butyl group remains a critical binding element by occupying a lipophilic domain in the kinase which is exposed upon rearrangement of the activation loop. An aromatic ring attached to N-2 of the pyrazole nucleus provides important π-CH$_2$ interactions with the kinase. The role of groups attached through an ethoxy group to the 4-position of the naphthalene and directed into the ATP-binding domain is elucidated. Pharmacophores with good hydrogen bonding potential, such as morpholine, pyridine, and imidazole, shift the melting temperature of p38α by 16−17 °C translating into K_d values of 50−100 pM. Finally, we describe several compounds that potently inhibit TNF-α production when dosed orally in mice.

Introduction

The proinflammatory cytokines tumor necrosis factor-α (TNF-α) and interleukin-1β (IL-1β) contribute to the regulation of the body's response to infection and cellular stress.[1] However, chronic and excessive production of TNF-α and IL-1β are believed to underlie the progression of many autoimmune diseases such as rheumatoid arthritis (RA),[2] Crohn's disease, and psoriasis.[3] The chimeric TNF-α antibody, infliximab,[4,5] is approved for the treatment of RA and Crohn's disease, while the IL-1 receptor antagonist, anakinra,[6] and the soluble TNF-α receptor fusion protein, etanercept,[7−10] are approved for the treatment of RA. These reports confirm that cytokine regulation represents an important advance in antiinflammatory therapeutics. An alternate approach to controlling cytokine levels involves disruption of the signal transduction pathway leading to their release from stimulated-inflammatory cells. A key element in this pathway is p38 mitogen activated protein (MAP) kinase.[11] Activation of this kinase under a variety of cellular stresses results in bisphosphorylation on a Thr-Gly-Tyr motif located in the activation loop. Once activated, p38 phosphorylates and activates other kinases and transcription factors leading to stabilized mRNA and an increase or decrease in the expression of certain target genes.[12−15]

The discovery of pyridinyl imidazole **1** (SB 203580)[11] (Chart 1) as a potent (Table 1) and selective inhibitor of p38α and its use in several animal models of inflammation validated this kinase as an important antiinflammatory therapeutic target.[16−23] Analogues of **1**,[24,25] along with alternate structural types of compounds,[26] continue to be developed as antiinflammatory agents.

We recently described *N*-pyrazole-*N*-aryl urea **2**[27] as a modest inhibitor of p38α (Chart 1). Refining this lead compound to include a tolyl ring at N-2 of the pyrazole (i.e., **3**), replacing the 4-chlorophenyl ring with naphthalene (i.e., **4**), and attaching an ethoxy morpholine group furnished 1-(5-*tert*-butyl-2-*p*-tolyl-2*H*-pyrazol-3-yl)-3-[4-(2-morpholin-4-yl-ethoxy)naphthalen-1-yl]urea (BIRB 796, **5**) as a potent and selective inhibitor of p38α.[28] Recently, **5** was shown to inhibit in vivo LPS-stimulated TNF-α production in a human clinical trial.[29] Compound **5** has advanced into human clinical trials for the treatment of autoimmune diseases. One of the unique characteristics of the pyrazole aryl urea class of compounds is the binding kinetics to p38α: slow k_{on} and long k_{off} rates.[28] We can rationalize these results with X-ray crystallographic observations (Figure 1a). For this class of compounds to bind to p38α, the activation loop, consisting in part of conserved residues Asp168-Phe169-Gly170, must undergo a substantial conformational change. It is our belief this conformational change of the protein is likely the rate determining step in the slow binding of this class of compounds. In the binding conformation, the side chain phenyl ring of Phe169 moves about 10 Å (DFG-out conformation) and participates in a lipophilic interaction with the aryl portion of the inhibitor. This interaction helps secure the inhibitor to the kinase and also possibly contributes to the long k_{off} rates. The implementation of a molecular assay employing exchange curve binding kinetics for deter-

Chart 1

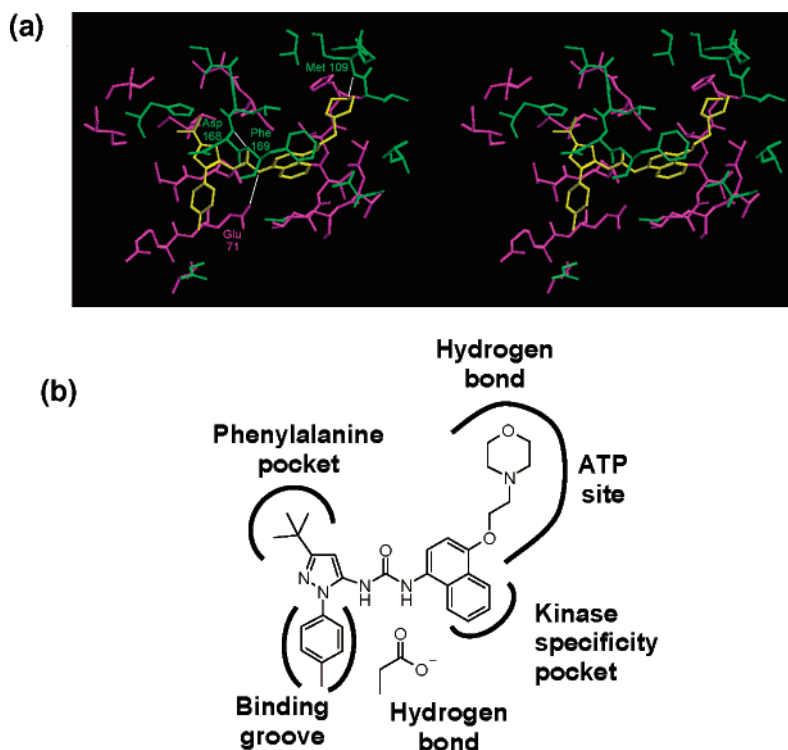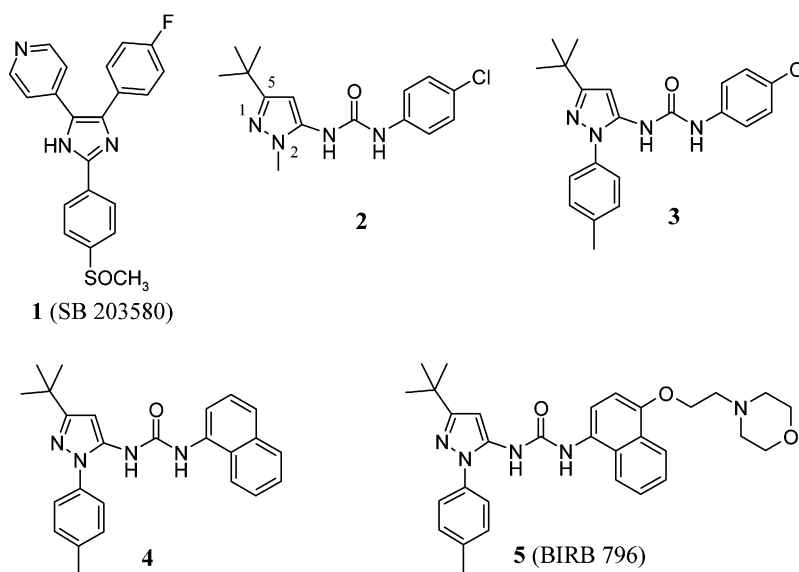**1** (SB 203580)

2

3

4

5 (BIRB 796)

Figure 1. (a) Stereoscopic view of the X-ray crystallographic complex of **5** (yellow) and human p38-α. Amino acid residues behind **5** are shown in magenta and those in front are displayed in green. (b) Summary of binding interactions of **5** and human p38-α.

mining K_d values was used in the discovery of **5**. This assay provides a better ranking of compounds with binding activities near the limit of our initial fluorescence-binding assay.[28] However, the labor intensity and accuracy for very potent binding compounds prevent the analysis of numerous target molecules using the exchange curve assay. For this reason, a method of determining p38α binding affinity relying on thermal denaturation was developed that has higher throughput and better accuracy for potent inhibitors.[30] In this case, K_d values are calculated from the denaturation temperature of the inhibitor/kinase complex. In this paper, we describe the thermal denaturation-derived binding affinity of analogues of **5** and correlate them to the binding mode observed from X-ray crystallography (Figure 1b).

The in vitro and in vivo TNF-α inhibition data for selected compounds are also shown.

Chemistry Section

Target molecules replacing the *tert*-butyl group at the 5-position of the pyrazole were prepared according to the procedure outlined in Scheme 1. Compound **11** was chosen as a representative example from Table 1. To affix a hydroxyl group to the *tert*-butyl moiety the substituted β-keto nitrile **8** was required. Silyl ether protection of methyl 2,2-dimethyl-3-hydroxypropionate (**6**) affords **7** and acetonitrile anion addition to the ester in hot toluene produces **8** with concomitant removal of the silyl protecting group. Pyrazole formation to furnish **9** is accomplished by heating **8** and *p*-tolylhydrazine in

Scheme 1[a]
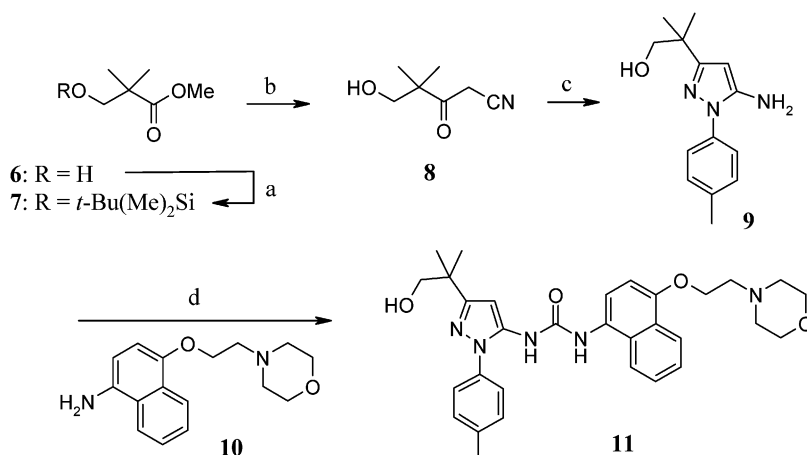
[a] Reagents: (a) *tert*-butyldimethylchlorosilane, imidazole, DMF; (b) NaH,acetonitrile, toluene, reflux; (c) *p*-tolylhydrazine hydrochloride, ethanol, reflux; (d) **10**, COCl$_2$, NaHCO$_3$, then **9**.

Scheme 2[a]
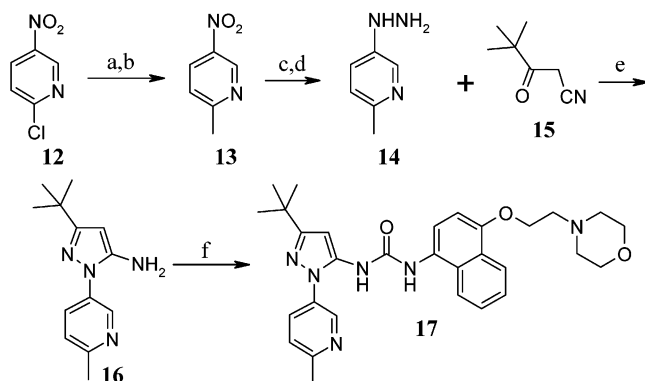
[a] Reagents: (a) Diethyl malonate, sodium, toluene; (b) HCl, heat; (c) H$_2$, Pd on carbon, 50 psi; (d) HCl, NaNO$_2$ then SnCl$_2$; (e) HCl, ethanol; (f) **10**, COCl$_2$, NaHCO$_3$, then **16**.

ethanol. The urea linkage is assembled from the phosgene-generated isocyanate of aminonaphthalene **10** and coupling with amine **9** to produce target molecule **11**.

Replacing the substitution at the N-2 position of the pyrazole requires hydrazines for condensation with β-keto-nitriles and subsequent urea formation as shown above. The synthesis of **17** as a representative example in Table 2 is outlined in Scheme 2. Treating 2-chloro-5-nitropyridine (**12**) with the anion of diethyl malonate followed by acid hydrolysis and decarboxylation provides 2-methyl-5-nitropyridine (**13**).[31] Reducing the nitro group of **13** with hydrogen and treating the amine with NaNO$_2$ and then SnCl$_2$ furnishes hydrazine **14**. Acid-catalyzed condensation of hydrazine **14** with β-keto-nitrile **15** gives amino pyrazole **16**. Urea formation to produce **17** is accomplished as before by reacting amino-naphthalene **10** with phosgene and base followed by **16**.

We have shown that the morpholine attached to the ethoxy linker makes an important contribution to the potency of **5**.[27] To further explore this observation, two routes were developed to produce analogues with other functionality appended to the ethoxy linker. In the first, amine-containing heterocycles are reacted with an iodoethoxy-naphthyl intermediate (i.e., **20**). As a representative example of Table 3, the synthesis of oxothiomorpholine analogue **25** is shown in Scheme 3. Base-catalyzed alkylation of naphthol **18** with 1-bromo-2-

chloroethane gives 2-chloroethoxy naphthalene **19**. Conversion of the chloroethoxy group to iodoethoxy **20** is accomplished with NaI, and subsequent treatment of **20** with thiomorpholine furnishes **21**. Oxidizing the thioether of **21** with NaIO$_4$ gives sulfoxide **22**, which upon exposure to TFA removes the Boc protecting group and provides aminonaphthalene **23**. Treatment of **23** with pyrazole-phenylcarbamate **24** in DMSO[32] gives target molecule **25**.
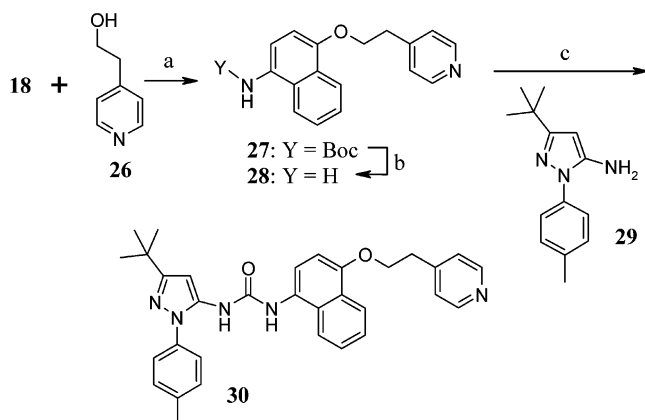
Alternatively, nonnucleophilic groups can be appended to the naphthol using Mitsunobu coupling conditions.[33] The synthesis of an example from Table 3, compound **30**, is shown in Scheme 4. Treatment of 2-pyridin-4-yl-ethanol (**26**) with naphthol **18** and triphenylphosphine and diethyl azodicarboxylate (DEADC) gives naphthyl ether **27**. Removal of the Boc protecting group of **27** with HCl provides aminonaphthalene **28**. The urea is formed by exposure of aminopyrazole **29** to phosgene and base and the subsequently produced isocyanate reacts with **28** to give target molecule **30**.

Results and Discussion

X-ray crystallographic data of **5** with human p38α (Figure 1a) reveals an important role for the *tert*-butyl group at C-5 of the pyrazole nucleus. This group occupies a lipophilic pocket (Phe169 pocket) between the two lobes of the kinase which is exposed upon reorganization of the activation loop (DFG-out conformation). We previously demonstrated the important binding contribution of lipophilic groups attached to C-5 of the pyrazole ring of a *N*-pyrazole-*N*-phenyl urea (i.e., **3**).[27] A similar set of modifications to an *N*-pyrazole-*N*-naphthyl urea (i.e., **33**) was examined to verify the essentiality of the *tert*-butyl group. Table 1 shows the thermal denaturation temperature (T_m) of the inhibitor and murine p38α complex[34] along with the calculated K_d value. The analogue lacking any lipophilic group at C-5 (**31**) shows a T_m result with p38α near the *apo*-protein value indicating a very weak binding compound. Introducing an *iso*-propyl group (**32**) raises the T_m of the ligand/kinase complex by nearly eight degrees or nearly 900-fold in binding affinity compared to **31** and is similar in binding potency to **1**. Increasing the size of the group at C-5 to a *tert*-butyl group (**33**) provides an even higher T_m and hence stronger binding affinity.

Scheme 3[a]
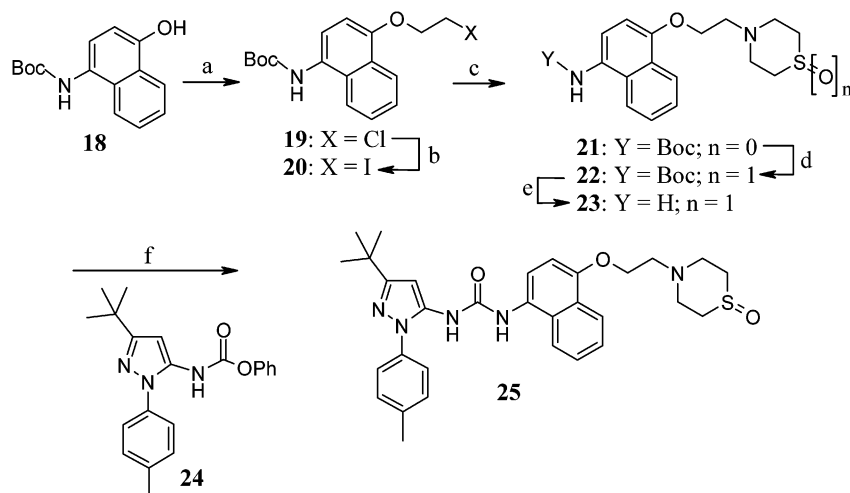
[a] Reagents: (a) 1-bromo-2-chloroethane, K_2CO_3; (b) NaI, acetone; (c) thiomorpholine, DIPEA; (d) $NaIO_4$, ethanol; (e) TFA; (f) **24**, DMSO.

Scheme 4[a]

[a] Reagents: (a) DEADC, PPh_3; (b) HCl; (c) **29**, $COCl_2$; $NaHCO_3$, then **28**.

Table 1. Substitution at C-5 of Pyrazole

Comp. number	R	T_m (°C)	Calc. K_d (nM)
apo-p38	---	46.6	---
1	(SB 203580)	54.9	20 ± 3[b]
11	---	53.0	56 ± 39[a]
31	H	49.1	2400 ± 640[a]
32	Me₂CH	56.6	3.4 ± 1.1[a]
33	Me₃C	61.0	0.23 ± 0.11[a]
34	cyclohexyl-Me	58.1	1.9 ± 0.3[b]

[a] Calculated from the equations in ref 30. [b] Calculated from T_m = 3.08(log K_a) + 31.2.

However, the larger cyclohexyl analogue (**34**) loses three degrees of thermal stability with p38α or nearly 10-fold of binding affinity compared to **33** and may reflect a size limitation in the protein for **33** vs **34**. Introducing a hydroxy group in this portion of the inhibitor (i.e., **11**) substantially reduces binding affinity consistent with the lipophilic character of this domain in p38α.

Substitution at N-2 of the pyrazole nucleus in the *N*-pyrazole-*N*-phenyl urea class of p38α inhibitors also has an important role in defining biological activity. The phenyl ring at N-2 of **5** interacts in a lipophilic π-CH_2 mode with the alkyl side chain of Glu71 and may also act as a water shield for the extensive hydrogen bond network of the urea atoms with the protein (Figure 1b). To further probe this particular region of the inhibitor, a series of derivatives of **5** were prepared. As seen in Table 2, replacing the phenyl ring in **33** with either methyl (**35**), cyclohexyl (**36**), or benzyl (**37**) results in a decrease of several degrees of thermal stability of the ligand/kinase complex. Small polar substituents attached to a phenyl ring (anilines **38** and **40**) and substituted pyridines (**17** and **42**) were generally tolerated compared to **33**. However, acylation of anilines **38** and **40** produces compounds (**39** and **41**) whose enzyme complexes are between 3 and 7 degrees less thermally
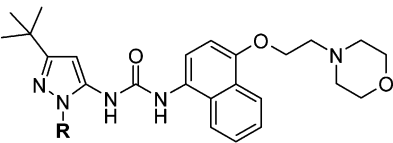
stable. The tolyl group (**5**) provides the best thermal stability when complexed with p38α.

We previously demonstrated that attaching an ethoxy-morpholine group to the naphthalene of **4**, to furnish **5**, greatly improves binding affinity by forming a hydrogen bond between the morpholine oxygen and the ATP-binding domain of p38α (Figure 1a,b).[27] Table 3 shows the results of examining other hydrogen bond accepting pharmacophores attached through an ethoxy linker to the 4-position of the naphthalene that access the ATP-binding domain. Support for the importance of this hydrogen bond is seen by the substantial decrease in thermal stability with piperidine (**43**), piperazine (**44**), and thiomorpholine (**47**) replacements for morpholine. Small lipophilic groups adjacent to the morpholine oxygen can affect the T_m values. For example, *cis*-dimethyl analogue **45** loses several degrees of thermal stability compared to **5**, indicating a potential steric interaction with the protein backbone that is not

Table 2. Substitution at N-2 of Pyrazole

comp no.	R	T_m (°C)	calc K_d (nM)
5	4-CH$_3$-phenyl	63.5	0.046 ± 0.025[a]
17	2-CH$_3$-pyridin-5-yl	61.3	0.18 ± 0.03[b]
33	phenyl	61.0	0.23 ± 0.11[a]
37	benzyl	53.4	64 ± 10[b]
35	methyl	54.5	26 ± 30[a]
36	cyclohexyl	54.8	23 ± 4[b]
38	3-NH$_2$-phenyl	60.9	0.23 ± 0.04[b]
39	3-NHAc-phenyl	55.9	9.9 ± 1.6[b]
40	4-NH$_2$-phenyl	61.4	0.16 ± 0.03[b]
41	4-NHAc-phenyl	53.4	64 ± 10[b]
42	2-CH$_3$O-pyridin-5-yl	59.1	0.87 ± 0.14[b]

[a] Calculated from the equations in ref 30. [b] Calculated from T_m = 3.08(log K_a) + 31.2.

observed with *trans*-dimethyl compound **46**. Aromatic hydrogen bond accepting moieties, such as 4-pyridine (**30**) and imidazole (**50**), provide T_m values with p38α comparable to morpholine (**5**). The location of the hydrogen-accepting atom in the ring is also important. Positional pyridine isomer **48** is 2.5 degrees less thermally stable when complexed with p38α than **30** indicating an erosion of the strength of the hydrogen bond. Replacement of morpholine with other hydrogen bond accepting pharmacophores,[35] such as thiomorpholine oxide and dimethoxyphenyl, produces analogues **25** and **49** with significantly lower thermal stability compared to **5**. These results, when taken together, emphasize the requirement for a hydrogen bond accepting pharmacophore to achieve tight binding with this class of compounds. Groups such as piperazine, piperidine, and thiomorpholine, do not participate in any protein interactions judging by their similar T_m values compared to **4**. However, analogues with good hydrogen bond accepting pharmacophores, such as morpholine (**5**), pyridine (**30**), and imidazole (**50**), achieve very strong binding affinities with p38α with T_m values between 62 and 63 °C, which translate into K_d values of 50−100 pM.

Selected compounds were further profiled for their ability to inhibit TNF-α production in LPS-stimulated THP-1 cells, human whole blood (HWB) and when orally dosed in mice. The results are shown in Table 4. The compounds inhibit TNF-α release in THP-1 cells with EC$_{50}$ values ranging from 10 to 65 nM and in HWB with EC$_{50}$ values of 440−3400 nM. The physicochemical properties of this class of inhibitors can affect the relative potency in the cellular assays. For example, **17** shows similar cellular inhibition compared to **5**, despite weaker binding affinity. The lower lipophilicity of **17** (log P = 3.6) vs **5** (log P = 4.6) likely reduces nonspecific lipophilic binding interactions with cellular and plasma proteins. In addition, THP-1 cellular potency for compounds with strong binding affinities (i.e., **5**, **30**, and **50**) may be underrepresented due to the potential limits of this assay. Most of the compounds significantly inhibit TNF-α production when administered orally to mice at 30 mg/kg with the more lipophilic compounds achieving high plasma concentrations. However, the less lipophilic compounds (i.e., **17**, **38**, **40**, and **50**) tended toward lower plasma levels compared to **5**.

Conclusion

We have described the SAR of **5**, a potent inhibitor of p38 that has advanced into human clinical trials. The thermal stability of the ligand:kinase complex provided the basis for determining the binding affinity for this class of compounds. The *tert*-butyl group of **5** is a critical binding element occupying a lipophilic domain in the kinase. An aromatic ring attached to N-2 of the pyrazole nucleus provides the best π-CH$_2$ interactions with the alkyl portion of the side chain of Glu71. Of those examined, a tolyl group provides the optimum binding affinity. We elucidated the role of a pharmacophore attached through an ethoxy group to the 4-position of the naphthalene and directed into the ATP-binding domain. Groups lacking hydrogen bond potential do not achieve any significant protein interactions. However, morpholine, pyridine, and imidazole are effective hydrogen bond acceptors for this class of compounds and facilitate very tight binding with the kinase. Finally, several of the compounds potently inhibit TNF-α production when dosed orally in an LPS-stimulated mouse.

Experimental Section

All solvents and reagents were obtained from commercial sources and used without further purification unless indicated otherwise. Melting points were obtained from a Mel-temp 3.0 or Fisher-Johns melting point apparatus and are uncorrected. ^{1}H NMR spectra were recorded on either a Bruker AC−F-270 spectrometer or Bruker Avance DPX 400 spectrometer. Chemical shifts are reported in parts per million (δ) from the tetramethylsilane resonance in the indicated solvent. Mass spectra were obtained from a Finnigan-SSQ7000 spectrometer. Samples were generally introduced by particle beam and ionized with NH$_4$Cl. TLC analytical separations were conducted with E. Merck silica gel F-254 plates of 0.25 mm thickness and were visualized with UV or I$_2$. Flash chromatographies were performed according to the procedure of Still et al. (EM Science Kieselgel 60, 70−230 mesh). Elemental analyses were performed at Quantitative Technologies, Inc., Whitehouse, NJ.

1-[5-(2-Hydroxy-1,1-dimethylethyl)-2-*p*-tolyl-2*H*-pyrazol-3-yl]-3-[4-(2-morpholin-4-yl-ethoxy)-naphthalen-1-yl]-urea (11). A solution of methyl-2,2-dimethyl-3-hydroxypropionate **6** (4.22 g, 31.9 mmol), imidazole (3.26 g; 47.8 mmol), and *tert*-butyldimethylchlorosilane (5.77 g, 38.3 mmol) in anhydrous DMF (60 mL) was stirred under an inert atmosphere for 12 h, quenched with water (200 mL), and extracted three times with ether. The combined organic extracts were washed with water and brine and dried (MgSO$_4$). Removal of volatiles in vacuo afforded 8.25 g of **7** as colorless oil (quantitative yield) which was used without purification.

To a suspension of NaH (60% in mineral oil, 0.55 g, 13.7 mmol) in anhydrous toluene (17 mL) at reflux was added dropwise over 1 h a solution of ester **7** (2.44 g, 9.90 mmol) and acetonitrile (0.72 mL, 13.9 mmol) in toluene (8 mL). The mixture was heated at reflux for 5 h, cooled to ambient temperature, and diluted with aqueous HCl to pH ∼ 4, and extracted with ethyl acetate. The combined organic extracts were washed with brine and dried (Na$_2$SO$_4$). Removal of the volatiles in vacuo provided pale yellow oil **8** (1.10 g) which was used without further purification.

A mixture of **8** (0.50 g, 3.5 mmol) and *p*-tolylhydrazine hydrochloride (0.56 g, 3.5 mmol) in ethanol (20 mL) was refluxed for 18 h, cooled to room temperature, and diluted with saturated aqueous NaHCO$_3$ solution and ethyl acetate. The organic layer was washed with brine and dried (Na$_2$SO$_4$). Removal of the volatiles in vacuo provided **9** as an orange oil (0.69 g, 79%) which used without further purification.

To a mixture of **10** (0.26 g, 0.98 mmol) in CH$_2$Cl$_2$ (15 mL) and saturated aqueous NaHCO$_3$ solution (15 mL) at 0 °C was

Table 3. Morpholine Analogues of Compound 5
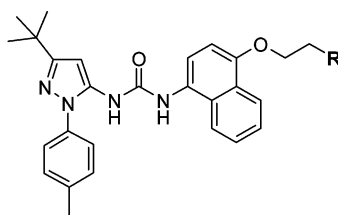
Comp. number	R	T_m (°C)	Calc. K_d (nM)	Comp. number	R	T_m (°C)	Calc. K_d (nM)
4	--	55.5	11 ± 3[a]	**46**	—N O (cis-2,6-dimethyl morpholine)	62.1	0.096 ± 0.016[b]
5	—N O (morpholine)	63.5	0.046 ± 0.025[a]				
25	—N S=O	60.2	0.40 ± 0.06[b]	**47**	—N S (thiomorpholine)	56.6	5.9 ± 0.9[b]
30	pyridine	62.4	0.10 ± 0.05[a]	**48**	pyridine	59.8	0.52 ± 0.08[b]
43	—N (piperidine)	55.4	14 ± 2[a]	**49**	OMe OMe (dimethoxyphenyl)	57.3	3.5 ± 0.6[b]
44	—N NH (piperazine)	55.6	12 ± 2[b]				
45	—N O (2,6-dimethyl morpholine)	58.4	1.5 ± 0.2[b]	**50**	—N N (imidazole)	62.4	0.074 ± 0.012[b]

[a] Calculated from the equations in ref 30. [b] Calculated from $T_m = 3.08(\log K_a) + 31.2$.

Table 4. In Vitro and In Vivo Activity of Selected Inhibitors

comp. no.	T_m (°C)	calc K_d (nM)	inhib. of TNF-α in THP-1 cells EC_{50} (nM)	inhib. of TNF-α in human whole blood EC_{50} (nM)	inhibition (%) of TNF-α in LPS-stimulated mice ($n = 6$) at		plasma levels (ng/mL) 90 min post dose at	
					30 mg/kg	10 mg/kg	30 mg/kg	10 mg/kg
5	63.5	0.046 ± 0.025[a]	18	780	84	63	75000	30000
17	61.3	0.18 ± 0.03[b]	19	530	87	86	54000	13000
25	60.2	0.40 ± 0.06[b]	50	1300	84	c	62800	
30	62.4	0.10 ± 0.05[a]	20	820	88	c	30000	
33	61.0	0.23 ± 0.11[a]	9	3400	81	57	38000	5400
38	60.9	0.23 ± 0.04[b]	11	1,600	c	NS[d]	c	1400
40	61.4	0.16 ± 0.03[b]	9	440	c	NS	c	ND[e]
42	59.1	0.87 ± 0.14[b]	42	>10000	40	c	80000	
46	62.1	0.096 ± 0.016[b]	16	770	50	NS	25000	4200
50	62.4	0.074 ± 0.012[b]	36	1100	81	c	7000	

[a] Calculated from the equations in ref 30. [b] Calculated from $T_m = 3.08(\log K_a) + 31.2$. [c] Not determined. [d] Not statistically significant. [e] Not detected.

added phosgene (20% in toluene, 1.5 mL, 2.9 mmol). The mixture was stirred 20 min and the organic layer dried (Na₂-SO₄). Most of the volatiles were removed in vacuo and **9** (0.24 g, 0.98 mmol) in anhydrous THF (7 mL) was added. The mixture was stirred at room temperature for 2 h. Removal of the volatiles in vacuo provided a residue which was purified by flash silica gel chromatography using 5% methanol in CH₂-Cl₂ as the eluent. Concentration in vacuo of the product-rich fractions provided a tan foam which was recrystallized from ether and hexanes to afford 30 mg of **11**. ¹H NMR (400 MHz, DMSO-*d₆*): δ 1.21 (s, 6 H, *gem*-di-Me), 2.40 (s, 3 H, *p*-Me), 2.54−2.57 (br m; 4 H), 2.84−2.87 (m, 2 H), 3.43 (d, 2 H, *J* = 5.6 Hz, CH₂−O), 3.58−3.61 (m, 4H), 4.25−4.28 (m, 2 H), 4.58 (t, 1 H, *J* = 5.6 Hz, OH), 6.35 (s, 1 H, pyrazole), 6.96 (d, 1 H, *J* = 8.5 Hz, aromatic), 7.36 (d, 2 H, *J* = 8 Hz, aromatic), 7.44 (d, 2 H, *J* = 8 Hz, aromatic), 7.52−7.62 (m, 3 H, aromatic), 7.88 (d, 1 H, *J* = 8 Hz, aromatic), 8.18 (d, 1 H, *J* = 9 Hz, aromatic), 8.57 (s, 1 H, urea), 8.74 (s, 1 H, urea); MS (ES⁺) *m/e* 544 (MH⁺); Anal. (C₃₁H₃₇N₅O₄) C, H, N.

1-[5-*tert*-Butyl-2-(6-methyl-pyridin-3-yl)-2*H*-pyrazol-3-yl]-3-[4-(2-morpholin-4-yl-ethoxy)-naphthalen-1-yl]-urea (17). A slurry of diethyl malonate (42 mL, 0.28 mol) and

sodium (4.71 g, 0.20 mol) was slowly warmed to 90 °C, stirred 2 h, heated to 120 °C for 30 min and cooled to room temperature. Toluene (200 mL) and 2-chloro-5-nitropyridine (**12**, 25.0 g, 0.16 mol) were added, and the slurry was heated at 110 °C for 1.5 h, cooled to room temperature, and stirred for 17 h. The volatiles were removed in vacuo, 6 N HCl (200 mL) was added, and the slurry heated to reflux for 4 h, cooled to room temperature, and neutralized with solid sodium carbonate. The mixture was extracted with ethyl acetate (6 × 100 mL) and the combined organic extracts were dried (MgSO₄). Removal of the volatiles in vacuo provided a solid which was purified by a plug of flash silica gel (2 × 2 in.) using 20% ethyl acetate in petroleum ether as the eluent. Concentration in vacuo of the product-rich fractions afforded 2-methyl-5-nitropyridine (**13**) as a tan solid (15.2 g, 70%). ¹H NMR (400 MHz, CDCl₃) δ 9.34 (s, 1H), 8.41 (m, 1H), 7.37 (m, 1H), 2.73 (s, 3H).

A mixture of **13** (13.0 g, 94.1 mmol) and 10% Pd/C (0.10 g) in 1,4-dioxane (150 mL) was hydrogenated at 50 psi using a Parr apparatus for 24 h and filtered over Celite. Removal of the volatiles in vacuo afforded 5-amino-2-methylpyridine (9.90 g, 97%) as a tan solid. This material was dissolved immediately

in 6 N HCl (100 mL), cooled to 0 °C, and vigorously stirred. Sodium nitrite (6.32 g, 91.6 mmol) in water (50 mL) was added. After 30 min, tin (II) chloride dihydrate (52.0 g, 230 mmol) in 6 N HCl (100 mL) was added, and the slurry was stirred at 0 °C for 3 h. The mixture was made basic with 40% aqueous KOH solution to pH 14 and extracted with ethyl acetate (6 × 250 mL). The combined organic extracts were dried (MgSO$_4$) and removal of the volatiles in vacuo afforded 5-hydrazino-2-methylpyridine (**14**) as a tan solid (8.0 g, 71%). A solution of **14** (8.0 g, 65.0 mmol) and 4,4-dimethyl-3-oxopentanenitrile (**15**, 10.0 g, 79.9 mmol) in ethanol (200 mL) containing 6 N HCl (6 mL) was refluxed for 17 h, cooled to room temperature, neutralized with NaHCO$_3$, and filtered. Removal of the volatiles in vacuo from the filtrate provided a residue which was purified with flash silica gel chromatography using ethyl acetate as the eluent. Concentration in vacuo of the product-rich fractions afforded 5-amino-3-*tert*-butyl-1-(2-methylpyridine-5-yl)pyrazole (**16**) as a tan solid (9.21 g, 62%). ^{1}H NMR (400 MHz, CDCl$_3$) δ 8.51 (s, 1H), 8.17 (m, 1H), 7.71 (s, 1H), 6.39 (s, 1H), 2.93 (s, 2 H), 2.57 (s, 3H), 1.37 (s, 9H).

To a 0 °C solution of **10** (0.40 g, 1.47 mmol) in CH$_2$Cl$_2$ (20 mL) and saturated aqueous NaHCO$_3$ (20 mL) was added phosgene (1.93 M in toluene, 1.50 mL). The mixture was stirred 15 min and the organic layer was dried (MgSO$_4$), and most of the volatiles were removed in vacuo. A solution of **16** (0.30 g, 1.30 mmol) in CH$_2$Cl$_2$ (10 mL) was added, and the mixture was stirred for 17 h at ambient temperature. Removal of the volatiles in vacuo provided a residue that was purified by flash silica gel chromatography using ethyl acetate then 10% methanol in ethyl acetate as the eluents. Concentration of the product-rich fractions afforded a colorless solid which was recrystallized from warm tetrahydrofuran/petroleum ether to give **17** as a colorless solid (0.65 g, 95%). mp 147−9°C. ^{1}H NMR (400 MHz, CDCl$_3$) δ 8.55 (s, 1H), 8.25 (m, 1H), 7.78 (s, 1H), 7.52 (m, 3H), 7.37 (d, $J = 8.2$ Hz, 1H), 7.05 (m, 3H), 6.70 (d, $J = 8.2$ Hz, 1H), 6.45 (s, 1H), 4.28 (t, $J = 5.6$ Hz, 2H), 3.78 (m, 4H), 2.99 (t, $J = 5.6$ Hz, 2H), 2.70 (m, 4H), 2.54 (s, 3H), 1.34 (s, 9H). Anal. (C$_{30}$H$_{36}$N$_6$O$_3$) C, H, N.

1-[5-*tert*-Butyl-2-*p*-tolyl-2*H*-pyrazol-3-yl]-3-[4-(2-(1-oxothiomorpholin-4-yl)ethoxy)naphthalen-1-yl]-urea (25). A suspension of (4-hydroxy-naphthalen-1-yl)carbamic acid *tert*-butyl ester (**18**, 7.0 g, 27 mmol), powdered K$_2$CO$_3$ (18.6 g, 139 mmol) and 1-bromo-2-chloroethane (7.74 g, 54 mmol) in acetonitrile (120 mL) was heated at 80 °C overnight, cooled to room temperature, and partitioned between ethyl acetate and water. The organic layer was washed with brine, dried (MgSO$_4$), and the volatiles removed in vacuo. Purification of the residue by flash chromatography using 25% ethyl acetate in hexanes as the eluent and concentration of the product-rich fractions in vacuo provided a solid which was triturated with 25% ethyl acetate in hexanes to afford 3.30 g (38%) of (4-(2-chloroethoxy)naphthalen-1-yl)carbamic acid *tert*-butyl ester (**19**). ^{1}H NMR (400 MHz, CDCl$_3$): δ 8.38 (d, 1H), 7.88 (d, 1H), 7.7−7.5 (m, 3H), 6.83 (d, 1H), 6.62 (bs, 1H), 4.42 (m, 2H), 4.01 (m, 2H), 1.58 (s, 9H). MS (CI): m/e 322 (MH$^+$).

A mixture of **19** (3.30 g, 10.2 mmol) and NaI (15 g, 102 mmol) in anhydrous acetone (30 mL) was heated at reflux for 64 h, cooled to room temperature, and diluted with CH$_2$Cl$_2$ and water. The organic layer was washed with water and brine and dried (Na$_2$SO$_4$). Removal of the volatiles in vacuo provided 4.03 g (94%) of (4-(2-iodoethoxy)naphthalen-1-yl)carbamic acid *tert*-butyl ester (**20**). ^{1}H NMR (400 MHz, CDCl$_3$): δ 8.41 (d, 1H), 7.93 (d, 1H), 7.7−7.5 (m, 3H), 6.81 (d, 1H), 6.55 (bs, 1H), 4.43 (m, 2H), 3.62 (m, 2H), 1.59 (s, 9H).

A mixture of **20** (1.0 g, 2.4 mmol), thiomorpholine (0.25 g, 2.4 mmol) and *N,N*-di-*iso*-propylethylamine (DIPEA) (0.42 mL, 2.4 mmol) in anhydrous DMF (5 mL) was heated at 40 °C overnight, cooled to room temperature, and diluted with ether and water. The organic layer was washed with water and brine and dried (MgSO$_4$). Removal of the volatiles in vacuo provided a residue which was purified by flash silica gel chromatography using 33% hexanes in ethyl acetate as the eluent. Concentration in vacuo of the product-rich fractions provided 0.73 g (78%) of (4-(2-thiomorpholin-4-yl-ethoxy)naphthalen-1-yl)carbamic acid *tert*-butyl ester (**21**). ^{1}H NMR (400 MHz, CDCl$_3$) δ 8.29 (d, 1H), 7.92 (d, 1H), 7.7−7.5 (m, 3H), 6.84 (d, 1H), 6.60 (bs, 1H), 4.41 (m, 2H), 3.08 (m, 6H), 2.78 (m, 4H), 1.58 (s, 9H).

To a 0−5 °C mixture of **21** (0.73 g, 1.87 mmol) in ethanol (50 mL) was added NaIO$_4$ (0.42 g, 1.95 mmol). The mixture was slowly warmed to room temperature, stirred overnight, and diluted with ethyl acetate and water. The organic layer was washed with water and brine and dried (MgSO$_4$). Removal of the volatiles in vacuo provided a residue which was purified by flash silica gel chromatography using 20% methanol in ethyl acetate as the eluent. Concentration in vacuo of the product-rich fractions provided 0.45 g (60%) of (4-(2-(1-oxo-thiomorpholin-4-yl)ethoxy)naphthalen-1-yl)carbamic acid *tert*-butyl ester (**22**). ^{1}H NMR (400 MHz, CDCl$_3$): δ 8.28 (d, 1H), 7.92 (d, 1H), 7.7−7.5 (m, 3H), 6.82 (d, 1H), 6.55 (bs, 1H), 4.33 (m, 2H), 3.35 (m, 2H), 3.12 (M, 2H), 2.95 (m, 6H), 1.58 (s, 9H).

A mixture of **22** (0.45 g, 1.1 mmol) and trifluoroacetic acid (0.63 g, 5.5 mmol) in CH$_2$Cl$_2$ (5 mL) was stirred at room temperature overnight and quenched with K$_2$CO$_3$ (0.76 g, 5.5 mmol). The mixture was filtered, and the volatiles were removed in vacuo to provide 1-amino-(4-(2-(1-oxo-thiomorpholin-4-yl)ethoxy)naphthalene (**23**) which was used without further purification.

A mixture of **23** (0.08 g, 0.26 mmol) and [5-*tert*-butyl-2-(4-methylphenyl)-2*H*-pyrazol-3-yl]-carbamic acid phenyl ester (prepared from **29** and phenyl chloroformate in pyridine and THF) (**24**, 0.14 g, 0.39 mmol) in anhydrous DMSO (1 mL) was heated at 40 °C overnight, cooled to room temperature, and diluted with ethyl acetate and water. The organic layer was washed with 2 N NaOH, water, and brine and dried (MgSO$_4$). Removal of the volatiles in vacuo provided a residue which was purified by flash silica gel chromatography using 20% methanol in ethyl acetate as the eluent. Concentration in vacuo of the product-rich fractions provided 0.05 g (34%) **25**. mp 182−4 °C. ^{1}H NMR (400 MHz, CDCl$_3$): δ 8.28 (m, 1H), 7.88 (m 1H), 7.55 (m, 1H), 7.41 (d, 1H), 7.12 (m, 2H), 7.02 (m, 2H), 6.79 (bs, 1H), 6.68 (d, 1H), 6.62 (bs, 1H), 6.36 (s, 1H), 4.28 (m,2H), 3.32 (m, 2H), 3.08 (m 2H), 2.90 (m, 6H), 2.33 (s, 3H), 1.36 (s, 9H). MS (CI): m/e 560 (MH$^+$). Anal. (C$_{31}$H$_{37}$N$_5$O$_3$S*0.5 H$_2$O); C, H, N.

1-(5-*tert*-Butyl-2-p-tolyl-2H-pyrazol-3-yl)-3-[4-(2-pyridin-4-yl-ethoxy)-naphthalen-1-yl]-urea (30). To a solution of **18** (0.509 g, 1.96 mmol), triphenylphosphine (1.52 g, 5.81 mmol) and 4-(2-hydroxyethyl)pyridine (**26**, 0.710 g, 5.77 mmol) in THF (10 mL) was added dropwise diethyl azodicarboxylate (DEADC) (0.90 mL, 5.72 mmol). The mixture was stirred overnight, and the volatiles were removed in vacuo. Purification of the residue by flash silica gel chromatography using ethyl acetate as the eluent and concentration in vacuo of the product-rich fractions provided [4-(2-pyridin-4-yl-ethoxy)-naphthalen-1-yl]-carbamic acid *tert*-butyl ester (**27**) contaminated with triphenylphosphine oxide. ^{1}H NMR (400 MHz, CDCl$_3$): δ 8.58 (m, 2H), 8.20 (d, 1H), 7.90 (d, 1H), 7.7−7.4 (m, 3H), 7.35 (d,1H), 7.21 (s, 1H), 6.84 (d, 1H), 6.72 (bs, 1H), 4.43 (t, 2H), 3.29 (t, 2H), 1.57 (s, 9H). MS (EI): m/e 365 (MH$^+$).

A solution of **27** (0.32 g) and HCl (5 mL of a 4.0 M solution in dioxane) in THF (10 mL) was stirred 3 h. The solid was filtered and dried in vacuo to provide 0.30 g (99%) of solid 4-(2-pyridin-4-yl-ethoxy)-naphthalen-1-ylamine dihydrochloride (**28**). MS (EI): m/e 265 (MH$^+$).

To a 0−5 °C mixture of 1-(4-methylphenyl)-3-(1,1-dimethylethyl)-5-aminopyrazole (**29**, 0.202 g, 0.88 mmol) in 15 mL of CH$_2$Cl$_2$ and 15 mL of saturated NaHCO$_3$ was added phosgene (0.5 mL of a 1.9 M solution in toluene; 0.97 mmol). The mixture was stirred rapidly for 15 min and the organic layer dried (Na$_2$SO$_4$). Removal of most of the volatiles in vacuo provided a residue which was added to a solution of **28** (0.280 g, 0.83 mmol) and DIPEA (0.52 mL) in THF (10 mL). The mixture was stirred overnight and filtered. The filtrate was concentrated in vacuo, and the residue was purified by flash silica gel chromatography using 25% hexanes in ethyl acetate as the eluent. Concentration in vacuo of the product-rich fraction provided a solid which was recrystallized with ethyl acetate

and methanol to provide 0.075 g (16%) of **30**. mp 187−90 °C. ^{1}H NMR (400 MHz, CDCl$_3$): δ 8.53 (d, 2H), 8.13 (d, 1H), 7.82 (d, 1H), 7.48 (m, 4H), 7.36 (d, 1H), 7.13−6.93 (m, 5H), 6.82 (bs, 1H), 6.68 (d, 1H), 6.45 (s, 1H), 4.42 (t, 2H), 3.25 (t, 2H), 2.24 (s, 3H), 1.35 (s, 9H). MS (EI): *m/e* 520 (MH$^+$). Anal. (C$_{32}$H$_{33}$N$_5$O$_2$) C, H, N.

1-[4-(2-Morpholin-4-yl-ethoxy)-naphthalen-1-yl]-3-(2-phenyl-*2H*-pyrazol-3-yl)-urea (31). mp 173−4 °C; ^{1}H NMR (400 MHz, DMSO-d$_6$): δ 2.54−2.56 (br m; 2 H), 2.84−2.87 (m, 2 H), 3.58−3.61 (m, 4H), 4.25−4.28 (m, 2 H), 6.46 (d, 1 H, *J* = 2 Hz), 6.96 (d, 1 H, *J* = 8 Hz, aromatic), 7.46−7.49 (m, 1 H, aromatic), 7.50−7.60 (m, 8 H, aromatic), 7.88 (d, 1 H, *J* = 8 Hz, aromatic), 8.18 (d, 1 H, *J* = 8 Hz, aromatic), 8.67 (s, 1 H, urea), 8.76 (s, 1 H, urea); MS (NH$_3$−CI) *m/e* 458 (MH$^+$); Anal. (C$_{26}$H$_{27}$N$_5$O$_3$*0.1C$_3$H$_8$O) C, H, N.

1-(5-*iso*-Propyl-2-phenyl-*2H*-pyrazol-3-yl)-3-[4-(2-morpholin-4-yl-ethoxy)-naphthalen-1-yl]-urea (32). mp 177−8 °C. ^{1}H NMR (400 MHz, DMSO-d$_6$): δ 1.23 (d, 6 H), 2.54−2.56 (br m; 4 H), 2.84−2.86 (m, 2 H), 2.87−2.94 (m, 1 H), 3.58−3.61 (m, 4H), 4.25−4.28 (m, 2 H), 6.34 (s, 1 H, pyrazole), 6.96 (d, 1 H, *J* = 8 Hz, aromatic), 7.42−7.47 (m, 1 H, aromatic), 7.52−7.61 (m, 7 H, aromatic), 7.88 (d, 1 H, *J* = 8 Hz, aromatic), 8.18 (d, 1 H, *J* = 8 Hz, aromatic), 8.64 (s, 1 H, urea), 8.77 (s, 1 H, urea); MS (PB−NH$_3$CI) *m/e* 500 (MH$^+$); Anal. (C$_{29}$H$_{33}$N$_5$O$_3$) C, H, N.

1-(5-*tert*-Butyl-2-phenyl-*2H*-pyrazol-3-yl)-3-[4-(2-morpholin-4-yl-ethoxy)-naphthalen-1-yl]-urea (33). mp 107−10 °C. ^{1}H NMR (400 MHz, DMSO-d$_6$): δ 1.28 (s, 9 H, *tert*-Bu), 2.54−2.56 (br m; 4 H), 2.84−2.87 (m, 2 H), 3.58−3.60 (m, 4H), 4.25−4.28 (m, 2 H), 6.38 (s, 1 H, pyrazole), 6.97 (d, 1 H, *J* = 8 Hz, aromatic), 7.41−7.47 (m, 1 H, aromatic), 7.52−7.61 (m, 7 H, aromatic), 7.89 (d, 1 H, *J* = 8 Hz, aromatic), 8.17 (d, 1 H, *J* = 9 Hz, aromatic), 8.63 (s, 1 H, urea), 8.77 (s, 1 H, urea); MS (PB−NH$_3$CI) *m/e* 514 (MH$^+$); Anal. (C$_{30}$H$_{35}$N$_5$O$_3$) C, H, N.

1-[5-(1-Methylcyclohexyl)-2-phenyl-*2H*-pyrazol-3-yl]-3-[4-(2-morpholin-4-yl-ethoxy)-naphthalen-1-yl]-urea (34). mp 147−149 °C. ^{1}H NMR (400 MHz, DMSO-d$_6$): δ 1.20 (s, 3 H), 1.44−1.50 (br m, 8 H), 1.98−2.00 (m, 2 H), 2.54−2.56 (br m; 4 H), 2.84−2.87 (m, 2 H), 3.59−3.61 (m, 4H), 4.25−4.28 (m, 2 H), 6.36 (s, 1 H, pyrazole), 6.96 (d, 1 H, *J* = 8 Hz, aromatic), 7.42−7.45 (m, 1 H, aromatic), 7.52−7.61 (m, 7 H, aromatic), 7.90 (d, 1 H, *J* = 8 Hz, aromatic), 8.18 (d, 1 H, *J* = 8 Hz, aromatic), 8.62 (s, 1 H, urea), 8.76 (s, 1 H, urea); MS (ES$^+$) *m/e* 554 (MH$^+$); Anal. (C$_{33}$H$_{39}$N$_5$O$_3$) C, H, N.

1-(5-*tert*-Butyl-2-methyl-*2H*-pyrazol-3-yl)-3-[4-(2-morpholin-4-yl-ethoxy)-naphthalen-1-yl]-urea (35). mp 201−2 °C. ^{1}H NMR (400 MHz, DMSO-d$_6$) δ 9.07 (s, 1H), 8.89 (s, 1H), 8.21 (m, 2H), 7.99 (m, 1H), 7.75 (m, 2H), 7.67 (m, 1H), 6.11 (s, 1H), 3.67 (s, 3H), 3.46 (m, 4H), 2.51 (m, 2H), 2.39 (m, 4H), 1.72 (m, 2H), 1.45 (s, 9H). Anal. (C$_{25}$H$_{33}$N$_5$O$_3$) C, H, N.

1-(5-*tert*-Butyl-2-cyclohexyl-*2H*-pyrazol-3-yl)-3-[4-(2-morpholin-4-yl-ethoxy)-naphthalen-1-yl]-urea (36). mp 216−7 °C. ^{1}H NMR (400 MHz, DMSO-d$_6$) δ 8.81 (s, 1H), 8.21 (m, 3H), 7.99 (m, 1H), 7.75 (m, 2H), 7.67 (m, 1H), 6.25 (s, 1H), 3.61 (m, 1H), 3.49 (m, 4H), 2.47 (m, 2H), 2.41 (m, 4H), 2.25−1.72 (m, 12H), 1.45 (s, 9H). Anal. (C$_{30}$H$_{41}$N$_5$O$_3$) C, H, N.

1-(2-Benzyl-5-*tert*-butyl-*2H*-pyrazol-3-yl)-3-[4-(2-morpholin-4-yl-ethoxy)-naphthalen-1-yl]-urea (37). Mp: 180−1 °C; ^{1}H NMR (400 MHz, DMSO-d$_6$): δ 1.23 (s, 9 H, tert-Bu), 2.54−2.57 (br m; 4 H), 2.84−2.87 (m, 2 H), 3.59−3.61 (m, 4H), 4.26−4.29 (m, 2 H), 5.24 (s, 1 H, pyrazole), 6.97 (d, 1 H, *J* = 8 Hz, aromatic), 7.11 (d, 2 H, *J* = 7 Hz, aromatic), 7.28 (d, 1 H, *J* = 7 Hz, aromatic), 7.36 (t, 2 H, *J* = 2 Hz, aromatic), 7.52−7.63 (m, 3 H, aromatic), 7.92 (d, 1 H, *J* = 8 Hz, aromatic), 8.19 (d, 1 H, *J* = 8 Hz, aromatic), 8.57 (s, 1 H, urea), 8.68 (s, 1 H, urea); MS (NH$_3$−CI) *m/e* 528 (MH$^+$); Anal. (C$_{31}$H$_{37}$N$_5$O$_3$) C, H, N.

1-[2-(3-Aminophenyl)-5-*tert*-butyl-*2H*-pyrazol-3-yl]-3-[4-(2-morpholin-4-yl-ethoxy)-naphthalen-1-yl]urea (38). To a 0 °C solution of phenyl chloroformate (1.6 mL; 12 mmol) in THF (30 mL) was added dropwise a solution of 2-(3-nitrophenyl)-5-*tert*-butyl-2*H*-pyrazol-3-yl-amine (2.5 g; 9.6 mmol) and pyridine (1.1 mL; 13 mmol) in THF (10 mL). The mixture was stirred at room temperature overnight and diluted with

ethyl acetate and water. The organic layer was washed with brine and dried. Removal of the volatiles in vacuo provided a solid which was triturated with hot 10% ethyl acetate and petroleum ether (80 mL). The solid was filtered and dried to furnish 2.5 g (67%) of [5-*tert*-butyl-2-(3-nitro-phenyl)-2*H*-pyrazol-3-yl]-carbamic acid phenyl ester. ^{1}H NMR (270 MHz, DMSO-d$_6$) δ 8.38 (s, 1H), 8.24 (d, 1H), 8.10 (d, 1H), 7.85 (t, 1H), 7.40 (m, 2H), 7.25−7.1 (m, 4H), 6.48 (s, 1H), 1.36 (s, 9H).

A solution of [5-*tert*-butyl-2-(3-nitro-phenyl)-2*H*-pyrazol-3-yl]-carbamic acid phenyl ester (2.49 g; 6.5 mmol), **10** (1.43 g; 5.2 mmol) and DIPEA (2.28 mL; 13.1 mmol) in anhydrous DMSO (55 mL) was stirred at room temperature for 2 days and diluted with ethyl acetate (10 mL) and brine (150 mL). The solid was filtered and recrystallized with ethyl acetate, THF and methanol to afford 1.87 g (64%) of 1-[2-(3-nitrophenyl)-5-*tert*-butyl-2*H*-pyrazol-3-yl]-3-[4-(2-morpholin-4-yl-ethoxy)-naphthalen-1-yl]-urea. mp 200−2 °C. ^{1}H NMR (270 MHz, DMSO-d$_6$) δ 8.80 (m, 1H), 8.46 (s, 1H), 8.3−8.1 (m, 4H), 7.85 (m, 2H), 7.52 (m, 3H), 6.95 (d, 1H), 6.42 (s, 1H), 4.28 (m, 2H), 3.60 (m, 4H), 2.84 (m, 2H), 2.55 (m, 4H), 1.33 (s, 9H).

To a refluxing solution of 1-[2-(3-nitrophenyl)-5-*tert*-butyl-2*H*-pyrazol-3-yl]-3-[4-(2-morpholin-4-yl-ethoxy)-naphthalen-1-yl]-urea (0.33 g) in ethanol (10 mL) was added 10% Pd on carbon (0.33 g) and ammonium formate (0.23 g). The mixture was heated for 1.5 h, cooled to room temperature and filtered over Celite. The volatiles were removed in vacuo to provide 0.31 g (100%) of **38**. ^{1}H NMR (270 MHz, DMSO-d$_6$) δ 8.86 (s, 1H), 8.62 (s, 1H), 8.19 (d, 1H), 7.93 (d, 1H), 7.66 (d, 1H), 7.55 (m, 2H), 7.18 (t, 1H), 6.97 (d, 1H), 6.73 (s, 1H), 6.64 (m, 2H), 6.35 (s, 1H), 5.44 (bs, 2H), 4.27 (t, 2H), 3.60 (m, 4H), 2.86 (m, 2H), 2.55 (m, 4H), 1.27 (s, 9H).

***N*-[3-(3-*tert*-Butyl-5-{3-[4-(2-morpholin-4-yl-ethoxy)-naphthalen-1-yl]-ureido}-pyrazol-1-yl)-phenyl]acetamide (39).** To a solution of acetyl chloride (0.25 µL, 0.3 mmol) in THF (5 mL) was added a solution of **38** (0.15 g; 0.3 mmol) and pyridine (28 µL, 0.3 mmol) in THF (2 mL). The mixture was stirred overnight and diluted with ethyl acetate and water. The organic layer was washed with brine and dried. Removal of the volatiles in vacuo provided a residue which was purified by flash silica gel chromatography using ethyl acetate as the eluent. Concentration in vacuo of the product-rich fractions provided 0.089 g (54%) of **39**. ^{1}H NMR (270 MHz, DMSO-d$_6$) δ 10.2 (s, 1H), 8.79 (s, 1H), 8.69 (s, 1H), 8.20 (d, 1H), 7.93 (d, 1H), 7.81 (s, 1H), 7.65−7.48 (m, 4H), 7.45 (t, 1H), 7.23 (d, 1H), 6.97 (d, 1H), 6.36 (s, 1H), 4.28 (t, 2H), 3.60 (m, 4H), 2.85 (m, 2H), 2.56 (m, 4H), 2.08 (s, 3H), 1.28 (s, 9H). MS (CI) *m/e* 571 (MH$^+$).

1-[2-(4-Aminophenyl)-5-*tert*-butyl-*2H*-pyrazol-3-yl]-3-[4-(2-morpholin-4-yl-ethoxy)-naphthalen-1-yl]urea (40). Prepared in a manner similar to **38**. ^{1}H NMR (270 MHz, DMSO-d$_6$) δ 8.83 (s, 1H), 8.45 (s, 1H), 8.19 (d, 1H), 7.90 (d, 1H), 7.65−7.4 (m, 5H), 7.13 (d, 1H), 6.96 (d, 1H), 6.70 (d, 1H), 6.30 (s, 1H), 5.41 (m, 2H), 4.28 (m, 2H), 3.61 (m, 4H), 2.86 (m 2H), 2.55 (m, 4H), 1.28 (s, 9H).

***N*-[4-(3-*tert*-Butyl-5-{3-[4-(2-morpholin-4-yl-ethoxy)-naphthalen-1-yl]-ureido}-pyrazol-1-yl)-phenyl]acetamide (41).** Prepared in a manner similar to **39**. ^{1}H NMR (270 MHz, DMSO-d$_6$) δ 10.1 (s, 1H), 8.79 (s, 1H), 8.59 (s, 1H), 8.18 (d, 1H), 7.90 (d, 1H), 7.75 (s, 1H), 7.61−7.5 (m, 5H), 7.47 (t, 1H), 6.96 (d, 1H), 6.35 (s, 1H), 4.28 (t, 2H), 3.59 (m, 4H), 2.85 (m, 2H), 2.56 (m, 4H), 2.09 (s, 3H), 1.27 (s, 9H). MS (CI) *m/e* 571 (MH$^+$).

1-[5-*tert*-Butyl-2-(6-methoxypyridin-3-yl)-*2H*-pyrazol-3-yl]-3-[4-(2-morpholin-4-yl-ethoxy)-naphthalen-1-yl]-urea (42). Prepared in a manner similar to **17**. mp 108−110 °C. ^{1}H NMR (400 MHz, CDCl$_3$) δ 8.35 (s, 1H), 8.21 (m, 1H), 7.75 (s, 1H), 7.58 (m, 4H), 7.41 (d, *J* = 8.1 Hz, 1H), 7.08 (d, *J* = 8.1 Hz, 2H), 6.76 (d, *J* = 8.1 Hz, 1H), 6.49 (s, 1H), 4.25 (t, *J* = 5.6 Hz, 2H), 3.97 (s, 3H), 3.75 (m, 4H), 2.94 (t, *J* = 5.6 Hz, 2H), 2.67 (m, 4H), 1.37 (s, 9H). Anal. (C$_{30}$H$_{36}$N$_6$O$_4$) C, H, N.

1-(5-*tert*-Butyl-2-*p*-tolyl-*2H*-pyrazol-3-yl)-3-[4-(2-piperidin-1-yl-ethoxy)-naphthalen-1-yl]-urea (43). A solution of 4-amino-1-naphthol (3.12 g, 16.0 mmol), di-*tert*-butyl dicarbonate (3.49 g, 16.0 mmol), triethylamine (6.7 mL, 48.0 mmol)

and DMAP (0.3 g) in anhydrous THF (50 mL) was stirred at room temperature for 2 days and diluted with ethyl acetate and water. The organic layer was washed with saturated NaHCO$_3$ and brine and dried (MgSO$_4$). Removal of the volatiles in vacuo provided a residue which was purified by flash silica gel chromatography using 33% ethyl acetate in hexanes as the eluent. Concentration in vacuo of the product-rich fractions provided 2.55 g (58%) of carbonic acid 4-amino-naphthalen-1-yl ester *tert*-butyl ester. MS (CI): *m/e* 260 (MH$^+$)

To a 0–5 °C mixture of **29** (0.746 g, 3.24 mmol) in 60 mL of CH$_2$Cl$_2$ and 60 mL of saturated NaHCO$_3$ was added phosgene (6.7 mL of a 1.9 M solution in toluene; 12.9 mmol). The mixture was stirred rapidly for 15 min, and the organic layer was dried (MgSO$_4$). Removal of most of the volatiles in vacuo provided a residue which was added to a solution of carbonic acid 4-amino-naphthalen-1-yl ester *tert*-butyl ester (0.811 g, 2.95 mmol) in 25 mL THF. The mixture was stirred overnight and the volatiles were removed in vacuo. The residue was purified by flash silica gel chromatography using 25% ethyl acetate in hexanes as the eluent. Concentration in vacuo of the product-rich fractions provided 1.37 g (66%) of carbonic acid *tert*-butyl ester 4-[3-(5-*tert*-butyl-2-p-tolyl-2*H*-pyrazol-3-yl)-ureido]-naphthalen-1-yl ester. MS (CI): *m/e* 515 (MH$^+$), 415 (MH–BOC).

A solution of carbonic acid *tert*-butyl ester 4-[3-(5-*tert*-butyl-2-p-tolyl-2*H*-pyrazol-3-yl)-ureido]-naphthalen-1-yl ester (0.56 g) in 7 mL of CH$_2$Cl$_2$ and 2 mL of trifluoroacetic acid (TFA) was stirred at room-temperature overnight and the volatiles removed in vacuo. The residue was diluted with ethyl acetate and washed with saturated NaHCO$_3$ and brine and dried (MgSO$_4$). Removal of the volatiles in vacuo provided 1-(5-*tert*-butyl-2-p-tolyl-2H-pyrazol-3-yl)-3-(4-hydroxy-naphthalen-1-yl)-urea which was used without further purification. MS (CI): *m/e* 415 (MH$^+$).

A mixture of 1-(5-*tert*-butyl-2-p-tolyl-2*H*-pyrazol-3-yl)-3-(4-hydroxy-naphthalen-1-yl)-urea (0.123 g, 0.297 mmol), 1-(2-chloroethyl)piperidine hydrochloride (0.060 g, 0/327 mmol), NaOH (0.98 mL of a 1 M solution, 0.98 mmol) and *N*-benzyl-tri-butylammonium chloride (0.03 mmol) in 3 mL of water and 2 mL of CH$_2$Cl$_2$ was heated at 50 °C for 8 h, cooled to room temperature, diluted with ethyl acetate, washed with water and brine. and dried (MgSO$_4$). Removal of the volatiles in vacuo provided a residue which was purified by flash silica gel chromatography using 23% methanol in ethyl acetate as the eluent. Concentration in vacuo of the product-rich fractions provided 0.055 g (35%) of **43**. mp 96–98 °C. ^{1}H NMR (270 MHz, CDCl$_3$): δ 8.25 (dd, 1H), 7.79 (m, 1H), 7.44 (m, 2H), 7.25 (m, 1H), 7.0–6.5 (m, 7H), 6.40 (s, 1H), 4.25 (m, 2H), 2.95 (m, 2H), 2.64 (m, 4H), 2.27 (s, 3H), 1.68 (m, 4H), 1.47 (m, 2H), 1.28 (s, 9H). MS (EI): *m/e* 526 (MH$^+$). Anal. (C$_{32}$H$_{39}$N$_5$O$_2$) C, H; N: calcd, 13.32; found, 12.66.

1-(5-*tert*-Butyl-2-*p*-tolyl-2*H*-pyrazol-3-yl)-3-[4-(2-piper-azin-1-yl-ethoxy)-naphthalen-1-yl]urea Dihydrochloride (44). Prepared in a manner similar to **43**. mp 190 °C (dec). ^{1}H NMR (400 MHz, DMSO-*d*$_6$): δ 9.64 (bs, 2H), 9.07 (s, 1H), 8.89 (s, 1H), 8.32 (d, 1H), 8.02 (d, 1H), 7.68 (d, 1H), 7.56 (m, 2H), 7.45 (d, 2H), 7.34 (d, 2H), 7.00 (d, 2H), 6.38 (s, 1H), 4.60 (bs, 2H), 2.08 (s, 3H), 1.27 (s, 9H). MS (CI): *m/e* 527 (MH$^+$). Anal. (C$_{33}$H$_{41}$N$_5$O$_3$*2HCl*2H$_2$O); C; H: calcd, 6.98; found, 6.49; N: calcd, 13.22; found,12.73.

1-(5-*tert*-Butyl-2-*p*-tolyl-2*H*-pyrazol-3-yl)-3-{4-[2-((2S,-6R)-2,6-dimethylmorpholin-4-yl)-ethoxy]naphthalen-1-yl}urea (45). Prepared in a manner similar to **25**. mp 153–4 °C. ^{1}H NMR (400 MHz, DMSO-*d*$_6$): δ 8.79 (s, 1H), 8.58 (s, 1H), 8.15 (d, 1H), 7.88 (d, 1H), 7.65–7.35 (m, 7H), 6.96 (d, 1H), 6.33 (s, 1H), 4.23 (m 2H), 3.58 (m, 2H), 2.85 (m, 4H), 2.37 (s, 3H), 1.80 (m, 2H), 1.29 (s, 9H), 1.05 (d, 6H). MS (CI): *m/e* 556 (MH$^+$). Anal. (C$_{33}$H$_{41}$N$_5$O$_3$); C, H, N.

1-(5-*tert*-Butyl-2-*p*-tolyl-2*H*-pyrazol-3-yl)-3-{4-[2-((2S,-6S)-2,6-dimethylmorpholin-4-yl)-ethoxy]naphthalen-1-yl}urea (46). Prepared in a manner similar to **25**. mp 137–9 °C. ^{1}H NMR (400 MHz, DMSO-*d*$_6$): δ 8.78 (s, 1H), 8.57 (s, 1H), 8.18 (d, 1H), 7.88 (d, 1H), 7.65–7.35 (m, 7H), 6.95 (d, 1H), 6.36 (s, 1H), 4.28 (m 2H), 3.92 (m, 2H), 2.79 (m, 2H), 2.58 (m 2H),

2.39 (s, 3H), 2.22 (m, 2H), 1.28 (s, 9H), 1.12 (d, 6H). MS (CI): *m/e* 556 (MH$^+$). Anal. (C$_{33}$H$_{41}$N$_5$O$_3$*H$_2$O); C, H, N.

1-(5-*tert*-Butyl-2-*p*-tolyl-2*H*-pyrazol-3-yl)-3-[4-(2-thio-morpholin-4-yl-ethoxy)-naphthalen-1-yl]urea (47). Prepared in a manner similar to **25**. mp 122–4 °C. ^{1}H NMR (400 MHz, DMSO-*d*$_6$): δ 8.75 (s, 1H), 8.53 (s, 1H), 8.18 (d, 1H), 7.88 (d, 1H), 7.6–7.3 (m, 7H), 6.95 (d, 1H), 6.35 (s, 1H), 4.24 (m 2H), 2.92 (m, 2H), 2.82 (m, 4H), 2.62 (m, 4H), 2.41 (s, 3H), 1.29 (s, 9H). MS (CI): *m/e* 544 (MH$^+$). Anal. (C$_{31}$H$_{37}$N$_5$O$_2$S); C, H, N.

1-(5-*tert*-butyl-2-p-tolyl-2H-pyrazol-3-yl)-3-[4-(2-pyridin-3-yl-ethoxy)-naphthalen-1-yl]-urea (48). Prepared in a manner similar to **30**. mp 166–8 °C. ^{1}H NMR (400 MHz, CDCl$_3$): δ 8.72 (s, 1H), 8.56 (d, 1H), 8.26 (d, 1H), 7.85 (d, 1H), 7.74 (d, 1H), 7.53 (m, 2H), 7.33 (m, 3H), 6.95–6.80 (m, 4H), 6.53 (bs, 1H), 6.42 (m, 2H), 4.38 (t, 2H), 3.32 (t, 2H), 2.23 (s, 3H), 1.33 (s, 9H). MS (EI): *m/e* 520 (MH$^+$). Anal. (C$_{32}$H$_{33}$N$_5$O$_2$) C, H, N.

1-(5-*tert*-Butyl-2-*p*-tolyl-2*H*-pyrazol-3-yl)-3-{4-[2-(3,4-dimethoxyphenyl)-ethoxy]-naphthalen-1-yl}urea (49). Prepared in a manner similar to **30**. mp 196–7 °C. ^{1}H NMR (400 MHz, DMSO-*d*$_6$): δ 8.75 (s, 1H), 8.58 (s, 1H), 8.20 (d, 1H), 7.88 (d, 1H), 7.65–7.35 (m, 7H), 7.03 (s, 1H), 6.95 (d, 1H), 6.88 (s, 2H), 6.35 (s, 1H), 4.32 (t, 2H), 3.73 (s, 3H), 3.70 (s, 3H), 3.12 (t, 2H), 2.39 (s, 3H), 1.28 (s, 9H). MS (CI): *m/e* 579 (MH$^+$). Anal. (C$_{35}$H$_{38}$N$_4$O$_4$*0.5H$_2$O); C, H, N.

1-(5-*tert*-butyl-2-*p*-tolyl-2*H*-pyrazol-3-yl)-3-[4-(2-imida-zol-1-yl-ethoxy)-naphthalen-1-yl]-urea (50). To a solution of **18** (0.341 g, 1.24 mmol), triphenylphosphine (0.975 g, 3.72 mmol) and 1-(2-hydroxyethyl)imidazole (0.417 g, 3.72 mmol) in THF (6 mL) was added dropwise DEADC (0.59 mL, 3.72 mmol). The mixture was stirred overnight and the volatiles were removed in vacuo. Purification of the residue with flash silica gel chromatography using 9% methanol in ethyl acetate as the eluent and concentration in vacuo of the product-rich fractions provided a solid. Trituration of the solid with ether and drying in vacuo provided 0.291 g (64%) of [4-(2-imidazol-1-yl-ethoxy)-naphthalen-1-yl]-carbamic acid *tert*-butyl ester. ^{1}H NMR (270 MHz, CDCl$_3$): δ 8.20 (d, 1H), 7.88 (d, 1H), 7.72–7.5 (m, 6H), 7.13 (bs,1H), 6.74 (d, 1H), 4.50 (d, 2H), 4.42 (m, 2H), 1.54 (s, 9H). MS (EI): *m/e* 354 (MH$^+$).

A solution of [4-(2-imidazol-1-yl-ethoxy)-naphthalen-1-yl]-carbamic acid *tert*-butyl ester (0.283 g) in CH$_2$Cl$_2$ (6 mL) and TFA (1.5 mL) was stirred at room temperature overnight. Removal of the volatiles in vacuo provided a residue which was diluted with ethyl acetate, washed with saturated NaH-CO$_3$ and brine, and dried (MgSO$_4$). Removal of the volatiles in vacuo provided 0.182 g (94%) of the solid 4-(2-imidazol-1-yl-ethoxy)-naphthalen-1-ylamine which was used without further purification.

To a 0–5 °C mixture of **29** (0.178 g; 0.778 mmol) in 7 mL of CH$_2$Cl$_2$ and 7 mL of saturated NaHCO$_3$ was added phosgene (1.2 mL of a 1.9 M solution in toluene; 2.33 mmol). The mixture was stirred rapidly for 20 min, and the organic layer was dried (MgSO$_4$). Removal of most of the volatiles in vacuo provided a residue which was added to a solution of 4-(2-imidazol-1-yl-ethoxy)-naphthalen-1-ylamine (0.179 g; 0.708 mmol) in 5 mL THF. The mixture was stirred overnight and diluted with ether. The solid was filtered and recrystallized from ethyl acetate to provide 0.10 g (28%) of **50**. mp 201–2 °C. ^{1}H NMR (270 MHz, CDCl$_3$): δ 7.90 (d, 1H), 7.66 (s, 1H), 7.5–6.95 (m, 12H), 6.57 (d, 1H), 6.46 (s, 1H), 4.45 (m, 2H), 4.30 (m, 2H), 2.25 (s, 3H), 1.38 (s, 9H). MS (EI): *m/e* 507 (MH$^+$). Anal. (C$_{30}$H$_{32}$N$_6$O$_2$) C, H, N.

Biological Methods. 1. Thermal Denaturation Assay. The details of the thermal denaturation experiments is found in the preceding article in this issue.[30] Briefly, the UV thermal melt experiments were carried out using a Perkin-Elmer Lambda 40 spectrophotometer. For each measurement, a quartz cuvette was loaded with 2.5 µM murine p38α MAP kinase and 25 µM inhibitor in a pH 7.0 buffer containing 10 mM sodium phosphate, 100 mM NaCl, and 1mM TCEP. Absorbance data at 230 nm was collected as the temperature was scanned from 25 to 80 °C at a ramp rate of 0.2 °C/min.

The melting temperature for each sample was calculated as the maximum deflection point of the first derivative of the melting transition using the Perkin-Elmer Templab software (version 1.62). Generally, the reported T_m values have an average standard error of $\pm$ 0.5 °C and are the average of at least two experiments. The T_m values are converted into K_d values using the equation $T_m = 3.08(\log K_a) + 31.2$, where $K_a = 1/K_d$, unless otherwise noted. The error associated with K_d calculations using this equation is $\pm$ 16%. A further description of error propagation in this assay has been described.[30]

Procedures for the THP-1 cellular assay for inhibition of LPS-stimulated TNF-α production, data analysis, and the in vivo LPS challenge assay have been described.[27] Briefly, THP-1 cells were preincubated in the presence and absence of test compound for 30 min, 37 °C, 5% CO_2. Cell mixture was stimulated with LPS (Sigma L-2630, 1 μg/mL final) and incubation continued overnight (18–24 h) as above. Supernatant was analyzed for human TNF-α by a commercially available ELISA (Biosource KHC3012). Data from $n\geq2$ assays were combined and analyzed by nonlinear regression using a three parameter logistic model to obtain an EC_{50} value. Compound **5** was analyzed in each experiment and the 95% confidence intervals for the EC_{50} were between 16 and 22 nM.

2. Human Whole Blood TNF-α (HWB) Assay. This assay, performed in 96-well polypropylene plates, measures the ability of test compounds to inhibit the elaboration of TNF-α by human whole blood following stimulation ex vivo with LPS (*Escherichia coli* lipopolysaccharide 0111:B4). Each test well contained the following components: 15 μL of compound serially diluted in human type AB serum, 135 μL of freshly drawn heparinized human whole blood, and 15 μL of LPS diluted in PBS containing 10% human serum for a final concentration of 50 ng LPS/mL. The plates were incubated for 30 min at 37 °C prior to addition of LPS. Control wells on every plate contained no test compound, with and without LPS. Following addition of LPS to test and control wells, the plates were placed on a rotary shaker for 30 s and then incubated for 5 h at 37 °C. To harvest plasma, 100 μL of PBS was added to all wells, the plates centrifuged to pellet cells, and the diluted plasma removed for TNF-α quantitation by standard ELISA, DELFIA, or electrochemiluminescence assay methods. TNF-α in each test well was determined by signal interpolation from a TNF-α standard curve run on the same plate. Test compound EC_{50} values were determined by nonlinear curve fitting of the data from cross-plate duplicate 11-point concentration–response curves to a 4-parameter logistic equation. Composite EC_{50} values were the geometric mean of EC_{50} values determined in blood from at least three donors. The EC_{50} of a standard inhibitor was determined on 239 independent test days across 113 different blood donors and returned lower and upper one-standard deviation values that were 29 and 37% of the geometric mean EC_{50} value.

References

(1) Dinarello, C. A. Inflammatory cytokines: interleukin-1 and tumor necrosis factor as effector molecules in autoimmune diseases. *Curr. Opin. Immunol.* **1991**, *3*, 941–948.

(2) Foster, M. L.; Halley, F.; Souness, J. E. Potential of p38 inhibitors in the treatment of rheumatoid arthritis. *Drug News Perspect.* **2000**, *13*, 488–497.

(3) Feldmann, M.; Brennan, F. M.; Maini, R. N. Role of cytokines in rheumatoid arthritis. *Annu. Rev. Immunol.* **1996**, *14*, 397–440.

(4) Maini, R.; St. Clair, E. W.; Breedveld, F.; Furst, D.; Kalden, J.; Weisman, M.; Smolen, J.; Emery, P.; Harriman, G.; Feldmann, M.; Lipsky, P. Infliximab (chimeric anti-tumour necrosis factor alpha monoclonal antibody) versus placebo in rheumatoid arthritis patients receiving concomitant methotrexate: a randomised phase III trial. *Lancet* **1999**, *354*, 1932–1939.

(5) Present, D. H.; Rutgeerts, P.; Targan, S.; Hanauer, S. B.; Mayer, L.; van Hogezand, R. A.; Podolsky, D. K.; Sands, B. E.; Braakman, T.; DeWoody, K. L.; Schaible, T. F.; van Deventer, S. J. Infliximab for the treatment of fistulas in patients with Crohn's disease. *N. Engl. J. Med.* **1999**, *340*, 1398–1405.

(6) Bresnihan, B. The prospect of treating rheumatoid arthritis with recombinant human interleukin-1 receptor antagonist. *BioDrugs* **2001**, *15*, 87–97.

(7) Jarvis, B.; Faulds, D. Etanercept: a review of its use in rheumatoid arthritis. *Drugs* **1999**, *57*, 945–966.

(8) Garrison, L.; McDonnell, N. D. Etanercept: therapeutic use in patients with rheumatoid arthritis. *Ann. Rheum. Dis.* **1999**, *58 Suppl 1*, 65–169.

(9) Mease, P. J.; Goffe, B. S.; Metz, J.; VanderStoep, A.; Finck, B.; Burge, D. J. Etanercept in the treatment of psoriatic arthritis and psoriasis: a randomised trial. *Lancet* **2000**, *356*, 385–390.

(10) Carteron, N. L. Cytokines in rheumatoid arthritis: trials and tribulations. *Mol. Med. Today* **2000**, *6*, 315–323.

(11) Lee, J. C.; Laydon, J. T.; McDonnell, P. C.; Gallagher, T. F.; Kumar, S.; Green, D.; McNulty, D.; Blumenthal, M. J.; Heys, J. R.; Landvatter, S. W.; Strickler, J. E.; McLaughlin, M. M.; Siemens, I. R.; Fisher, S. M.; Livi, G. P.; White, J. R.; Adams, J. L.; Young, P. R. A protein kinase involved in the regulation of inflammatory cytokine biosynthesis. *Nature* **1994**, *372*, 739–746.

(12) Tibbles, L. A.; Woodgett, J. R. The stress-activated protein kinase pathways. *Cell. Mol. Life Sci.* **1999**, *55*, 1230–1254.

(13) Ono, K.; Han, J. The p38 signal transduction pathway. Activation and function. *Cell. Signalling* **2000**, *12*, 1–13.

(14) Lee, J. C.; Kassis, S.; Kumar, S.; Badger, A.; Adams, J. L. p38 mitogen-activated protein kinase inhibitors-mechanisms and therapeutic potentials. *Pharmacol. Ther.* **1999**, *82*, 389–397.

(15) Salituro, F. G.; Germann, U. A.; Wilson, K. P.; Bemis, G. W.; Fox, T.; Su, M. S. Inhibitors of p38 MAP kinase: therapeutic intervention in cytokine-mediated diseases. *Curr. Med. Chem.* **1999**, *6*, 807–823.

(16) Badger, A. M.; Bradbeer, J. N.; Votta, B.; Lee, J. C.; Adams, J. L.; Griswold, D. E. Pharmacological profile of SB 203580, a selective inhibitor of cytokine suppressive binding protein/p38 kinase, in animal models of arthritis, bone resorption, endotoxin shock and immune function. *J. Pharmacol. Exp. Ther.* **1996**, *279*, 1453–1461.

(17) Gao, F.; Yue, T. L.; Shi, D. W.; Christopher, T. A.; Lopez, B. L.; Ohlstein, E. H.; Barone, F. C.; Ma, X. L. p38 MAPK inhibition reduces myocardial reperfusion injury via inhibition of endothelial adhesion molecule expression and blockade of PMN accumulation. *Cardiovasc. Res.* **2002**, *53*, 414–422.

(18) Clark, W. M.; Lutsep, H. L. Potential of anticytokine therapies in central nervous system ischemia. *Expert Opin. Biol. Ther.* **2001**, *1*, 227–237.

(19) Du, Y.; Ma, Z.; Lin, S.; Dodel, R. C.; Gao, F.; Bales, K. R.; Triarhou, L. C.; Chernet, E.; Perry, K. W.; Nelson, D. L.; Luecke, S.; Phebus, L. A.; Bymaster, F. P.; Paul, S. M. Minocycline prevents nigrostriatal dopaminergic neurodegeneration in the MPTP model of Parkinson's disease. *Proc. Natl. Acad. Sci. U.S.A.* **2001**, *98*, 14669–14674.

(20) Junn, E.; Mouradian, M. M. Apoptotic signaling in dopamine-induced cell death: the role of oxidative stress, p38 mitogen-activated protein kinase, cytochrome *c* and caspases. *J. Neurochem.* **2001**, *78*, 374–383.

(21) Newton, R.; Holden, N. Inhibitors of p38 Mitogen-Activated Protein Kinase: Potential as Anti-inflammatory Agents in Asthma? *Biodrugs* **2003**, *17*, 113–129.

(22) Schultz, R. M. Potential of p38 MAP kinase inhibitors in the treatment of cancer. *Prog. Drug Res.* **2003**, *60*, 59–92.

(23) Pargellis, C.; Regan, J. Inhibitors of p38 mitogen-activated protein kinase for the treatment of rheumatoid arthritis. *Curr. Opin. Invest. Drugs* **2003**, *4*, 566–571.

(24) Adams, J. L.; Badger, A. M.; Kumar, S.; Lee, J. C. p38 MAP kinase: Molecular target for the inhibition of pro-inflammatory cytokines. *Prog. Med. Chem.* **2001**, *38*, 1–60.

(25) Jackson, P. F.; Bullington, J. L. Pyridinylimidazole based p38 MAP kinase inhibitors. *Curr. Top. Med. Chem.* **2002**, *2*, 1009–1018.

(26) Cirillo, P. F.; Pargellis, C. A.; Regan, J. The nondiaryl heterocycle classes of p38 MAP kinase inhibitors. *Curr. Top. Med. Chem.* **2002**, *2*, 1021–1035.

(27) Regan, J.; Breitfelder, S.; Cirillo, P.; Gilmore, T.; Graham, A. G.; Hickey, E. R.; Klaus, B.; Madwed, J.; Moriak, M.; Moss, N.; Pargellis, C. A.; Pav, S.; Proto, A.; Swinamer, A.; Tong, L.; Torcellini, C. Pyrazole urea-based inhibitors of p38 MAP kinase: From lead compound to clinical candidate. *J. Med. Chem.* **2002**, *45*, 2994–3008.

(28) Pargellis, C. A.; Tong, L.; Churchill, L.; Cirillo, P.; Gilmore, T.; Graham, A. G.; Grob, P. M.; Hickey, E. R.; Moss, N.; Pav, S.; Regan, J. Inhibition of p38 map kinase by utilizing a novel allosteric binding site. *Nat. Struct. Biol.* **2002**, *9*, 268−272.

(29) Branger, J.; van den Blink, B.; Weijer, S.; Madwed, J.; Bos, C. L.; Gupta, A.; Polmar, S. H.; Olszyna, D. P.; Hack, C. E.; van Deventer, S. J. H.; Peppelenbosch, M. P.; van der Poll, T. Anti-inflammatory effects of a p38 mitogen activated protein kinase inhibitor, BIRB 796 BS, during human endotoxemia. *J. Immunol.* **2002**, *168*, 4070−4077.

(30) Kroe, R. R.; Regan, J.; Proto, A.; Peet, G. W.; Roy, T.; Dickert, L.; Fuschetto, N.; Pargellis, C. A.; Ingraham, R. H. Thermal denaturation: A method to rank slow binding, high-affinity p38α MAP kinase inhibitors. *J. Med. Chem.* **2003**, *46*, 4669−4675.

(31) Liu, M. C.; Lin, T. S.; Sartorelli, A. C. A one-pot synthesis of 3-nitro- and 3,5-dinitro-2-picolines. *Synth. Comm.* **1990**, *20*, 2965−2970.

(32) Thavonekham, B. A practical synthesis of ureas from phenyl carbamates. *Synthesis* **1997**, 1189−1194.

(33) Mitsunobu, O. The use of diethyl azodicarboxylate and triphenylphosphine in the synthesis and transformation of natural products. *Synthesis* **1981**, 1−28.

(34) Human p38-α and murine p38-α differ by two amino acids: Leu47 to His47 and Thr262 to Ala262. We have shown that these differences have negligible effects on the binding affinity for this class of inhibitors (data not shown).

(35) Abraham, M. H.; Duce, P. P.; Prior, D. V.; Barratt, D. G.; Morris, J. J.; Taylor, P. J. Hydrogen bonding. Part 9. Solute proton donor and proton acceptor scales for use in drug design. *J. Chem. Soc., Perkin Trans. 2* **1989**, 1355−1375.